

A Classical Nernst Engine

Julian Stark,¹ Kay Brandner,¹ Keiji Saito,² and Udo Seifert¹

¹*II. Institut für Theoretische Physik, Universität Stuttgart, 70550 Stuttgart, Germany*

²*Department of Physics, Keio University, 3-14-1 Hiyoshi, Kohoku-ku, Yokohama, Japan 223-8522*

We introduce a simple model for an engine based on the Nernst effect. In the presence of a magnetic field, a vertical heat current can drive a horizontal particle current against a chemical potential. For a microscopic model invoking classical particle trajectories subject to the Lorentz force, we prove a universal bound $3 - 2\sqrt{2} \simeq 0.172$ for the ratio between maximum efficiency and Carnot efficiency. This bound, as the slightly lower one $1/6$ for efficiency at maximum power, can indeed be saturated for large magnetic field and small fugacity irrespective of the aspect ratio.

PACS numbers: 05.60.Cd, 05.70.Ln, 85.80.-b

Introduction.— The Nernst effect describes the emergence of an electrical voltage perpendicular to a heat current transversing an isotropic conductor in the presence of a constant magnetic field [1]. However, while Seebeck-based devices, for which the heat and the particle current are coupled without a magnetic field, have been the subject of intensive research efforts during the last decades [2–5], only a few attempts were made to utilize the Nernst effect for power generation [6–9]. This lack of interest may have been caused by the uncompetitive net efficiency of Nernst-based devices, which is inevitably suppressed by the energetic cost of the strong magnetic fields they require. New discoveries in the phenomenological theory of thermoelectric effects as well as recent experiments showing the accessibility of magnetic field strengths [10–13], however, cast new light on the topic of Nernst engines.

Benenti and co-workers showed by a quite general analysis within the framework of linear irreversible thermodynamics that breaking the microscopic time-reversal symmetry by a magnetic field could, in principle, increase thermoelectric efficiency such that even devices operating reversibly at finite power seem to be achievable [14]. Such an intriguing suggestion asks for a better understanding of coupled heat and particle transport in magnetic fields. First progress in this direction was recently achieved within the paradigmatic class of multi-terminal models, for which it turned out that current conservation implies much stronger bounds on the efficiency than the standard rules of linear irreversible thermodynamics [15, 16]. For the minimal case of three terminals, these bounds were even shown to be tight [17]. Since these models were based on general particle transmission probabilities without reference to any specific microscopic dynamics, they leave the necessary conditions for saturating these bounds open.

Simple mechanical models have led to remarkable insight into the microscopic mechanisms underlying heat and matter transport [18, 19], especially in the context of thermoelectric efficiency [20–22]. So far, the effect of a

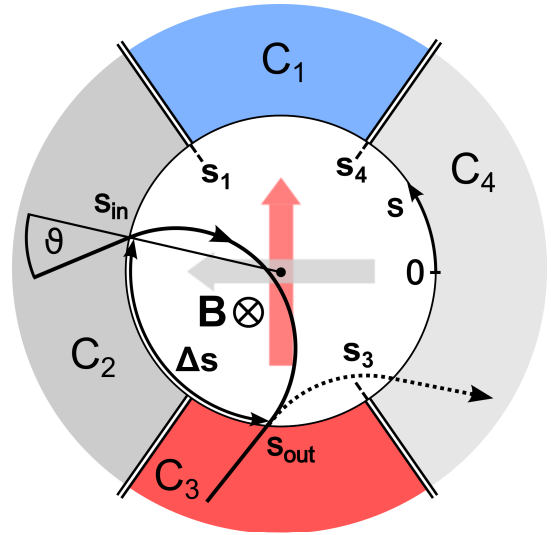


FIG. 1. Scheme of the classical Nernst engine. The vertical heat current (red arrow) between reservoir C_3 and C_1 with $T_3 > T_1$ drives a horizontal particle current (grey arrow) from reservoir C_4 to C_2 with $\mu_2 > \mu_4$. The bold black line denotes a classical trajectory leaving reservoir C_2 at s_{in} with an angle $\vartheta < 0$ and entering C_3 at s_{out} where $0 \leq s \leq 2\pi R$ parametrizes the circumference. The dotted line shows the corresponding time-reversed trajectory for an entry at s_{out} . For further symbols, see main text.

magnetic field breaking time-reversal symmetry on thermoelectric efficiency has not yet been addressed using such models. Nernst engines are ideal candidates to investigate the influence of broken time-reversal symmetry. We therefore propose a minimalistic, classical model for such an engine, which provides physical insight on the level of single particle trajectories.

System— Our classical system for studying transport is inspired by the Landauer-Büttiker approach, which has proven extremely useful in the quantum realm [23, 24]. As shown in Fig. 1, we consider a two-dimensional, circular and potential-free scattering region of radius R perpendicularly penetrated by a homogeneous magnetic field

\mathbf{B} of strength $B \equiv |\mathbf{B}|$, surrounded by four thermochemical reservoirs C_i . Due to the Lorentz force, a particle with energy E injected from reservoir C_i at s_{in} with an angle $\vartheta \in \Delta$, where $\Delta \equiv [-\pi/2, \pi/2]$, moves on a circle of radius

$$R_c = \sqrt{2mEc}/(|q|B) \equiv \nu(E)R \quad (1)$$

inside the scattering region. Here, c denotes the speed of light, $q < 0$ the charge of the particle and m its mass. This particle hits the boundary at a position $s_{\text{out}} \equiv s_{\text{in}} + \Delta s$. A simple geometrical analysis shows for the distance Δs measured along the boundary

$$\Delta s = 2R \begin{cases} g(\vartheta, \nu) + \pi & \text{for } \nu > 1, \sin \vartheta < -1/\nu \\ g(\vartheta, \nu) & \text{else} \end{cases} \quad (2)$$

with

$$g(\vartheta, \nu) \equiv \text{arccot}[(1 + \nu \sin \vartheta)/(\nu \cos \vartheta)]. \quad (3)$$

Note that from (2) onwards, we suppress in ν the dependence on the energy E to simplify the notation.

The fluxes entering and leaving the system through the reservoirs can be determined as follows. Any particle that reaches the circular boundary from one of the reservoirs is assumed to enter the scattering region. A Maxwell-Boltzmann statistics in reservoirs modeled as ideal gases with inverse temperature β_i and chemical potential μ_i then implies a total particle current

$$J_i^{\varrho+} \equiv \int_{l_i} ds \int_0^\infty dE \int_\Delta d\vartheta u_i(E) \cos \vartheta = \frac{\sqrt{2\pi m l_i}}{\beta_i^{3/2}} e^{\beta_i \mu_i} \quad (4)$$

flowing from the reservoir C_i with boundary length l_i into the system, where $u_i(E) \equiv \sqrt{2mE} \exp[-\beta_i(E - \mu_i)]$ [22]. Likewise, assuming that each particle hitting the boundary from inside the scattering region is absorbed in the adjacent reservoir, the steady-state current flowing into C_i reads

$$J_i^{\varrho-} \equiv \sum_j \int_{l_j} ds \int_0^\infty dE \int_\Delta d\vartheta u_j(E) \cos \vartheta \tau_i(E, s, \vartheta). \quad (5)$$

Note that we set Planck's constant as well as Boltzmann's constant equal to 1 throughout this letter. In (5), we have introduced the conditional probability $\tau_i(E, s, \vartheta)$ for a particle of energy E entering at position s with an angle ϑ to reach the boundary of the reservoir C_i after passing through the scattering region. Since we assume purely Hamiltonian dynamics, this probability can either be 1 or 0. In order to derive a concise expression for the net particle currents $J_i^\varrho \equiv J_i^{\varrho+} - J_i^{\varrho-}$, we define the transmission coefficients

$$\mathcal{T}_{ji}(E) \equiv \int_{l_i} ds \int_\Delta d\vartheta \tau_j(E, s, \vartheta) \cos \vartheta. \quad (6)$$

As our first main result, we can show that Liouville's theorem implies the sum rules [25]

$$\sum_i \mathcal{T}_{ji}(E) = 2l_j \quad \text{and} \quad \sum_j \mathcal{T}_{ji}(E) = 2l_i. \quad (7)$$

By combining (4), (5) and (7), we finally arrive at

$$J_i^\varrho = \sum_j \int_0^\infty dE \mathcal{T}_{ij}(E) (u_i(E) - u_j(E)). \quad (8)$$

An analogous calculation yields the net heat flux leaving reservoir C_i

$$J_i^q = \sum_j \int_0^\infty dE \mathcal{T}_{ij}(E) (E - \mu_i) (u_i(E) - u_j(E)). \quad (9)$$

Nernst Engine.— For a Nernst engine, we have to impose the boundary conditions

$$J_1^\varrho = J_3^\varrho = 0 \quad \text{and} \quad J_2^q = J_4^q = 0, \quad (10)$$

which ensure that the particle current occurs only horizontally and heat flows only vertically in the set-up of Fig. 1. From here on, we focus on the linear response regime. We choose the reference values, $\mu \equiv \mu_2$ and $T \equiv T_1$ and define $\Delta\mu_i \equiv \mu_i - \mu$ and $\Delta T_i \equiv T_i - T$. Linearizing the currents (8) and (9) with respect to ΔT_i and $\Delta\mu_i$ yields six phenomenological relations

$$J_i^\kappa = \sum_{j\nu} L_{ij}^{\kappa\nu} \mathcal{F}_j^\nu \quad \text{with} \quad \kappa, \nu = \varrho, q. \quad (11)$$

Here, we have introduced the affinities $\mathcal{F}_i^\varrho \equiv \Delta\mu_i/T$ and $\mathcal{F}_i^q \equiv \Delta T_i/T^2$, and the Onsager coefficients

$$\begin{pmatrix} L_{ij}^{\varrho\varrho} & L_{ij}^{\varrho q} \\ L_{ij}^{q\varrho} & L_{ij}^{qq} \end{pmatrix} \equiv \int_0^\infty dE u(E) \begin{pmatrix} 1 & E - \mu \\ E - \mu & (E - \mu)^2 \end{pmatrix} \times (2l_i \delta_{ij} - \mathcal{T}_{ij}(E)) \quad (12)$$

with $u(E) \equiv \sqrt{2mE} \exp[-\beta(E - \mu)]$. Using the constraints (10) to eliminate $\mathcal{F}_1^\varrho, \mathcal{F}_3^\varrho, \mathcal{F}_2^q$ and \mathcal{F}_4^q in (11) and defining the current vector $\mathbf{J} \equiv (J_4^\varrho, J_3^q)^t$ and the affinity $\mathcal{F} \equiv (\mathcal{F}_4^\varrho, \mathcal{F}_3^q)^t$ leaves us with

$$\mathbf{J} = \mathbb{L} \mathcal{F}, \quad \text{where} \quad \mathbb{L} \equiv \begin{pmatrix} L_{\varrho\varrho} & L_{\varrho q} \\ L_{q\varrho} & L_{qq} \end{pmatrix} \quad (13)$$

is a matrix of effective Onsager coefficients.

The role of geometry will be studied by introducing the aspect ratio $\mathcal{A} \equiv l_2/l_1$. For the choice $l_1 = l_3 = \pi R/(1 + \mathcal{A})$ and $l_2 = l_4 = \pi R\mathcal{A}/(1 + \mathcal{A})$, the resulting mirror symmetry implies

$$L_{\varrho q} = -L_{q\varrho}. \quad (14)$$

For a proper heat engine, we put $\Delta\mu_4 < 0$ and $\Delta T_3 > 0$. The generated output power and efficiency

then become $P = -\Delta\mu_4 J_4^g$ and $\eta = P/J_3^g$ [26]. Maximizing η with respect to \mathcal{F}_4^g under the condition $P \geq 0$ yields

$$\eta_{\max} = \eta_C \frac{1 - \sqrt{1 - \mathcal{Z}T}}{1 + \sqrt{1 - \mathcal{Z}T}} \quad \text{with} \quad \mathcal{Z}T \equiv \frac{L_{\rho q}^2}{\text{Det } \mathbb{L}}, \quad (15)$$

where $\eta_C \equiv 1 - T_1/T_3 \approx T\mathcal{F}_3^g$ denotes the Carnot efficiency. Obviously, like for conventional thermoelectric devices [14], the maximum efficiency depends only on a single dimensionless quantity, the thermomagnetic figure of merit $\mathcal{Z}T$. In the literature [1], this parameter is usually given in the form $\mathcal{Z}T = (NB)^2\sigma T/\kappa$, where NB is the thermomagnetic power, σ the electric and κ the thermal conductivity. However, this definition coincides with the one given in (15), if the transport coefficients NB, σ, κ are identified correctly with the effective Onsager coefficients [27]. In contrast to the naive expectation, NB is negative in our model, i.e., the net particle current flows from the right to the left in Fig. 1, although particles from the hot reservoir are deflected in the opposite direction. This feature is ultimately a consequence of the boundary conditions (10).

Two bounds successively constrain the parameter $\mathcal{Z}T$. First, since the second law requires the rate of entropy production $\dot{S} = \mathcal{F}^t \mathbf{J} = \mathcal{F}^t \mathbb{L} \mathcal{F}$ to be non-negative, the matrix \mathbb{L} must be positive semi-definite. Due to the symmetry (14), this condition reduces to $L_{\rho\rho}, L_{qq} \geq 0$. By recalling (15) one has [9]

$$0 \leq \mathcal{Z}T \leq 1. \quad (16)$$

Second, by techniques similar to the ones used in [16], we can show that the Hermitian matrix

$$\mathbb{K} \equiv \mathbb{L} + \mathbb{L}^t + i(\mathbb{L} - \mathbb{L}^t) \quad (17)$$

has to be positive semi-definite as a consequence of the sum rules (7) [25]. This constraint can be expressed as

$$(\text{Det } \mathbb{K})/4 = L_{\rho\rho}L_{qq} - L_{\rho q}^2 \geq 0, \quad (18)$$

leading to

$$0 \leq \mathcal{Z}T \leq 1/2. \quad (19)$$

Obviously, the constraint (19), which ultimately relies on Liouville's theorem, is stronger than (16). In particular, while the second law, in principle, allows the maximum efficiency to approach η_C in the limit $\mathcal{Z}T \rightarrow 1$, the bound (19) implies the significantly lower limit

$$\eta_{\max} \leq (3 - 2\sqrt{2})\eta_C \simeq 0.172\eta_C. \quad (20)$$

This universal bound on the efficiency of a classical Nernst engine is our second main result. It arises from the four-terminal set-up and the symmetry (14) but is independent of further details of the geometry and the

strength of the magnetic field. In the derivation of this bound, we have nowhere used that the trajectories are circular in the scattering region. Hence, it would also apply if an additional potential acted on the particles.

Quite generally, the existence of a bound provokes the question whether it can be saturated in any given microscopic model. For addressing this issue within our model, we need to determine the Onsager matrix \mathbb{L} and hence the transmission coefficients $\mathcal{T}_{ji}(E)$ explicitly.

Strong field regime.— Relation (2) allows to determine the $\mathcal{T}_{ji}(E)$ for any $E \geq 0$. However, the resulting expressions are quite involved [25]. We therefore begin with analyzing the limiting case $\nu \ll 1$. First, expanding (2) in ν yields

$$\Delta s = 2R\nu \cos\vartheta + \mathcal{O}(\nu^2). \quad (21)$$

Second, since this quantity is bounded from above by $\Delta s^* = 2R\nu \ll R$, we can consistently assume $\Delta s^* < \min\{l_1, l_2\}$, i.e., particles emitted from the reservoir C_i can either pass to the adjacent reservoir C_{i+1} or return to C_i . Consequently, we have $\mathcal{T}_{ji}(E) = 0$ for $j \neq i, i+1$. Moreover, the sum rules (7) require $\mathcal{T}_{ii}(E) = 2l_i - \mathcal{T}_{i+1i}(E)$. Hence, we are left with calculating $\mathcal{T}_{i+1i}(E)$. For this purpose, we recall Fig. 1 and recognize that a particle injected from the reservoir C_i at a certain position s_{in} must leap over the distance $\Delta s \geq s_i - s_{\text{in}}$ to reach reservoir C_{i+1} , where s_i marks the contact point of the reservoirs C_i and C_{i+1} . By virtue of (21), this transmission condition can be rewritten as $\vartheta_- < \vartheta < \vartheta_+$ with $\vartheta_{\pm} \equiv \pm \arccos[(s_i - s_{\text{in}})/(2R\nu)]$. Finally, by using the definition (6), we get

$$\mathcal{T}_{i+1i}(E) = \int_{s_i - \Delta s^*}^{s_i} ds_{\text{in}} \int_{\vartheta_-}^{\vartheta_+} d\vartheta \cos\vartheta = \pi R\nu(E). \quad (22)$$

Using the complete set of transmission coefficients $\mathcal{T}_{ji}(E)$ to calculate the primary Onsager coefficients (12) and taking into account the auxiliary conditions (10) yields, as our third main result, the effective Onsager matrix

$$\mathbb{L} = \frac{J_0}{2\sqrt{\pi}\mathcal{B}v} \begin{pmatrix} 1 & \sqrt{v-1}/\beta \\ -\sqrt{v-1}/\beta & (1+v)/\beta^2 \end{pmatrix}. \quad (23)$$

Here, we have defined $v \equiv 1 + (2 - \beta\mu)^2$ and the dimensionless strength of the magnetic field $\mathcal{B} \equiv |q|BR\sqrt{\beta}/(\sqrt{2}mc)$. The quantity $J_0 \equiv (2\pi)^{\frac{3}{2}}\sqrt{m}R \exp[\beta\mu]/\beta^{\frac{3}{2}}$ corresponds to the total particle current flowing into the scattering region at thermal equilibrium, i.e., for $\Delta T_i = \Delta\mu_i = 0$, as one can easily infer from (4).

The maximum efficiency in this strong field regime $\mathcal{B} \gg 1$ follows by inserting (23) into (15) as

$$\eta_{\max} = \eta_C \frac{\sqrt{2v} - \sqrt{1+v}}{\sqrt{2v} + \sqrt{1+v}} \quad \text{with} \quad \mathcal{Z}T = \frac{v-1}{2v}. \quad (24)$$

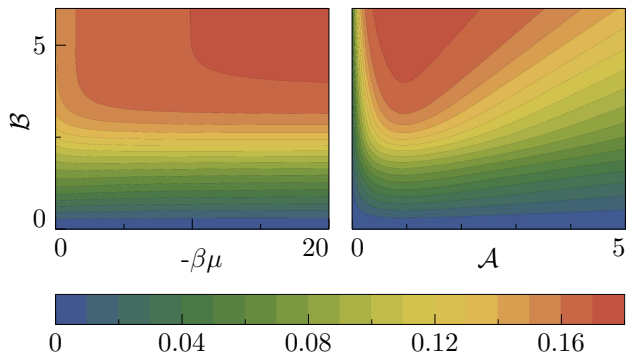


FIG. 2. Maximum efficiency. The left panel shows η_{\max}/η_C as a function of the rescaled magnetic field \mathcal{B} and $\beta\mu$ for aspect ratio $\mathcal{A} = 1$. The right panel shows the dependence on \mathcal{B} and \mathcal{A} for $\beta\mu = -20$.

The bounds (19) and (20) are indeed reached for $v \rightarrow \infty$, i.e., for $\beta\mu \rightarrow -\infty$ [28]. However, in this limit, the equilibrium current $J_0 \sim \exp[\beta\mu]$, and likewise the Onsager matrix (23), decay exponentially. Thus, the saturation of the bounds (19) and (20) comes at the price of vanishing power.

Efficiency diagrams.—Relaxing the assumption $\mathcal{B} \gg 1$, we now turn to an arbitrary field strength. By repeating the procedure outlined in the preceding section using the full relation (2) instead of the approximation (21) as a starting point, we obtain closed, analytical expressions for the transmission coefficients $\mathcal{T}_{ji}(E)$ now depending explicitly on \mathcal{B} and \mathcal{A} [25]. After evaluating the primary Onsager coefficients (12) numerically and including the boundary conditions (10), we calculate the maximum efficiency η_{\max} , which is plotted in Fig. 2. We find that, for any \mathcal{A} and $\beta\mu$, η_{\max} vanishes at $\mathcal{B} = 0$ as expected, since the vertical heat flux and the horizontal particle current decouple for vanishing magnetic field. As \mathcal{B} is increased, η_{\max} grows monotonically. Notably, if the aspect ratio deviates significantly from 1, larger values of \mathcal{B} are necessary for η_{\max} to approach its upper bound (20). This effect is readily understood by recalling that for the high field scenario to apply, $\Delta s \sim 1/\mathcal{B}$ for a typical trajectory must be smaller than $\min\{l_1, l_2\} = \pi R \min\{1, \mathcal{A}\}/(1+\mathcal{A})$ to ensure that only transitions between adjacent reservoirs are relevant. Our numerical results suggest an optimal aspect ratio $\mathcal{A}^*(\mathcal{B}, \beta\mu)$ close to 1. Exploring this issue in more detail will be left to future work.

Efficiency at maximum power.—After studying the maximum efficiency of our device, we now consider another important benchmark for the performance of a thermoelectric engine, its efficiency at maximum power η^* [26, 29–31], which is obtained by maximizing the output power $P = -\Delta\mu_4 J_4^o$ with respect to $\Delta\mu_4$. Expressed in terms of $\mathcal{Z}T$, this parameter reads

$$\eta^* \equiv \eta_{CA} \mathcal{Z}T / (2 - \mathcal{Z}T), \quad (25)$$

where $\eta_{CA} = \eta_C/2$ denotes the Curzon-Ahlborn value

[29], which is attained for $\mathcal{Z}T \rightarrow 1$. However, the constraint (19) implies the stronger bound

$$\eta^* \leq \eta_{CA}/3 \simeq 0.167\eta_C. \quad (26)$$

In the strong field regime, (25) becomes $\eta^* = \eta_{CA}(v - 1)/(3v + 1)$. Thus, like η_{\max} , η^* reaches the bound (26) only in the limit $v \rightarrow \infty$, i.e., for $\beta\mu \rightarrow -\infty$. We can refrain from showing numerical data for η^* , since they are practically the same as those for η_{\max} . Specifically, we have $0.97 < \eta^*/\eta_{\max} \leq 1$ throughout the whole parameter range of \mathcal{B} , \mathcal{A} and $\beta\mu$ due to $\eta_{\max} - \eta^* = (\mathcal{Z}T)^3/64 + \mathcal{O}((\mathcal{Z}T)^4)$.

Concluding perspectives.—In this letter, we have introduced a classical formalism to describe heat and particle transport in non-interacting systems, which can be regarded as the classical analogue to the well-established Landauer-Büttiker approach. The crucial quantities of this formalism are the energy-dependent transmission coefficients $\mathcal{T}_{ji}(E)$, for which we have proven the sum rules (7). We emphasize that these sum rules follow solely from Liouville’s theorem and thus hold for any kind of Hamiltonian dynamics inside a scattering region of arbitrary shape.

For a Nernst geometry, in which a heat current is coupled to a perpendicular particle current via a magnetic field, a universal bound significantly lower than the Carnot value constrains the maximum efficiency. This bound can indeed be saturated for a strong field and exponentially small fugacities in the reservoirs. The same bound holds for a cooling device based on the Ettingshausen effect [1], [32]. In both cases, this bound would not change even in the presence of an additional potential or for a geometrically deformed scattering region provided the two mirror symmetries are kept. It remains an open question, however, whether these bounds would also apply if one included inelastic scattering or particle-particle interactions. Finally, due to its simplicity and physical transparency, our classical approach can provide a valuable benchmark for assessing the role of quantum effects in future modeling.

U.S. acknowledges support from ESF through the EPSD network. K.S. was supported by MEXT (23740289).

-
- [1] H. J. Goldsmid, *Introduction to Thermoelectricity*, 1st ed. (Springer Series in Material Science, 2009).
 - [2] M. S. Dresselhaus, G. Chen, M. Y. Tang, R. Yang, H. Lee, D. Wang, Z. Ren, J.-P. Fleurial, and P. Gogna, *Adv. Mat.* **19**, 1043 (2007).
 - [3] G. J. Snyder and S. Toberer, *Nature Mater.* **7**, 105 (2008).
 - [4] L. E. Bell, *Science* **321**, 1457 (2008).
 - [5] C. J. Vineis, A. Shakouri, A. Majumdar, and M. G. Kanatzidis, *Adv. Mat.* **22**, 3970 (2010).
 - [6] J. F. Elliott, *J. Appl. Phys.* **30**, 1774 (1959).

- [7] D. A. Wright, *Brit. J. Appl. Phys.* **13**, 583 (1962).
- [8] M. H. Norwood, *J. Appl. Phys.* **34**, 594 (1963).
- [9] T. C. Harman and J. M. Honig, *J. Appl. Phys.* **34**, 189 (1963).
- [10] A. G. Pogosov, M. V. Budantsev, D. Uzur, A. Nogaret, A. E. Plotnikov, A. K. Bakarov, and A. I. Toropov, *Phys. Rev. B* **66**, 201303 (2002).
- [11] S. Maximov, M. Gbordzoe, H. Buhmann, L. W. Molenkamp, and D. Reuter, *Phys. Rev. B* **70**, 121308 (2004).
- [12] S. Goswami, C. Siegert, M. Pepper, I. Farrer, D. A. Ritchie, and A. Ghosh, *Phys. Rev. B* **83**, 073302 (2011).
- [13] J. Matthews, F. Battista, P. Samuelsson, and H. Linke, arXiv:1306.3694v1.
- [14] G. Benenti, K. Saito, and G. Casati, *Phys. Rev. Lett.* **106**, 230602 (2011).
- [15] K. Brandner, K. Saito, and U. Seifert, *Phys. Rev. Lett.* **110**, 070603 (2013).
- [16] K. Brandner and U. Seifert, arXiv:1308.2179v1, *New J. Phys.*, in press (2013).
- [17] V. Balachandran, G. Benenti, and G. Casati, *Phys. Rev. B* **87**, 165419 (2013).
- [18] C. Mejía-Monasterio, H. Larralde, and F. Leyvraz, *Phys. Rev. Lett.* **86**, 5417 (2001).
- [19] B. Li, G. Casati, and J. Wang, *Phys. Rev. E* **67**, 021204 (2003).
- [20] G. Casati, C. Mejía-Monasterio, and T. Prosen, *Phys. Rev. Lett.* **101**, 016601 (2008).
- [21] M. Horvat, T. Prosen, and G. Casati, *Phys. Rev. E* **80**, 010102(R) (2009).
- [22] K. Saito, G. Benenti, and G. Casati, *Chemical Physics* **375**, 508 (2010).
- [23] M. Büttiker, Y. Imry, R. Landauer, and S. Pinhas, *Phys. Rev. B* **31**, 6207 (1985).
- [24] M. Büttiker, *Phys. Rev. Lett.* **57**, 1761 (1986).
- [25] See supplemental material at [URL] for technical details.
- [26] U. Seifert, *Rep. Prog. Phys.* **75**, 126001 (2012).
- [27] The standard analysis [33] gives $\sigma = q^2 L_{ee}/T$ and $\kappa = \text{Det } \mathbb{L}/(T^2 L_{ee})$, where q is the charge of the particles. The thermomagnetic power is defined as the ratio $NB = V/\Delta T$ of the transverse voltage emerging due to a longitudinal temperature gradient ΔT if the transverse electrical current is held at 0 [1]. Putting $J_4^e = 0$ in (13) and solving for $V = -\Delta\mu_4/q$ gives $NB = V/\Delta T_3 = L_{eq}/(TqL_{ee})$.
- [28] The limit $\beta\mu \rightarrow +\infty$ is incompatible with our classical approach, since it would lead to an exponentially high equilibrium fugacity $\exp[\beta\mu]$ in the reservoirs [33].
- [29] F. L. Curzon and B. Ahlborn, *Am. J. Phys.* **43**, 22 (1975).
- [30] C. Van den Broeck, *Phys. Rev. Lett.* **95**, 190602 (2005).
- [31] M. Esposito, K. Lindenberg, and C. Van den Broeck, *Phys. Rev. Lett.* **102**, 130602 (2009).
- [32] To operate the model as a refrigerator, we have to choose $\Delta\mu_4$ such that, for $\Delta T_3 < 0$, $J_3^q > 0$. The performance of the resulting device is benchmarked by the coefficient $\varepsilon \equiv J_3^q/(\Delta\mu_4 J_4^q)$. Maximizing ε with respect to $\Delta\mu_4$ under the condition $J_3^q > 0$ yields
- $$\varepsilon_{\max} = \varepsilon_C \frac{1 - \sqrt{1 - \overline{ZT}}}{1 + \sqrt{1 - \overline{ZT}}}, \quad (27)$$
- where $\varepsilon_C \equiv -T/\Delta T_3$ denotes the coefficient of performance of an ideal refrigerator. As for the Nernst engine, the constraint (19) implies the bound $\varepsilon_{\max}/\varepsilon_C \leq 3 - 2\sqrt{2}$, which can be saturated only at the price of vanishing heat current within the high field limit.
- [33] H. B. Callen, *Thermodynamics and an Introduction to Thermostatistics*, 2nd ed. (John Wiley & Sons, New York, 1985).

SUPPLEMENTAL MATERIAL FOR A CLASSICAL NERNST ENGINE

Proof of the Sum Rules (7)

We will prove the sum rules

$$\sum_i \mathcal{T}_{ji}(E) = 2l_j \quad \text{and} \quad \sum_j \mathcal{T}_{ji}(E) = 2l_i \quad (1)$$

for the transmission coefficients $\mathcal{T}_{ji}(E)$ introduced in Eq. (6) of the main text. To this end, we consider a particle with fixed energy E injected at the position s_{in} and angle ϑ_{in} . After traveling through the circular scattering region the particle eventually leaves it at the position s_{out} and angle ϑ_{out} . Since we assume Hamiltonian dynamics inside the scattering region, there is a one-to-one mapping

$$\mathcal{M} : \begin{pmatrix} s_{\text{in}} \\ \vartheta_{\text{in}} \end{pmatrix} \mapsto \begin{pmatrix} s_{\text{out}} \\ \vartheta_{\text{out}} \end{pmatrix} = \begin{pmatrix} s_{\text{out}}(s_{\text{in}}, \vartheta_{\text{in}}) \\ \vartheta_{\text{out}}(s_{\text{in}}, \vartheta_{\text{in}}) \end{pmatrix}. \quad (2)$$

The conditional probability $\tau_j(s_{\text{in}}, \vartheta_{\text{in}})$, introduced in Eq. (5) of the main text, for a particle to reach the reservoir C_j for fixed initial conditions ϑ_{in} and s_{in} reads

$$\tau_j(s_{\text{in}}, \vartheta_{\text{in}}) = \int_{l_j} ds' \int_{-\pi/2}^{\pi/2} d\vartheta' \delta(s' - s_{\text{out}}) \delta(\vartheta' - \vartheta_{\text{out}}). \quad (3)$$

By recalling definition (6) of the main text,

$$\mathcal{T}_{ji}(E) \equiv \int_{l_i} ds_{\text{in}} \int_{-\pi/2}^{\pi/2} d\vartheta_{\text{in}} \tau_j(s_{\text{in}}, \vartheta_{\text{in}}) \cos \vartheta_{\text{in}}, \quad (4)$$

and using $\sum_j l_j = 2\pi R$ we obtain the first of the sum rules (1). To prove the second one, we change integration variables in (4) according to

$$\begin{pmatrix} s_{\text{in}} \\ \vartheta_{\text{in}} \end{pmatrix} \rightarrow \begin{pmatrix} s_{\text{out}} \\ \vartheta_{\text{out}} \end{pmatrix}, \quad (5)$$

thus ending up with

$$\sum_i \mathcal{T}_{ji} = \int_{-\pi/2}^{\pi/2} d\vartheta' \int_{l_j} ds' \int_0^{2\pi R} ds_{\text{out}} \int_{-\pi/2}^{\pi/2} d\vartheta_{\text{out}} \delta(s' - s_{\text{out}}) \delta(\vartheta' - \vartheta_{\text{out}}) \cos[\vartheta_{\text{in}}(s_{\text{out}}, \vartheta_{\text{out}})] J(s_{\text{out}}, \vartheta_{\text{out}}), \quad (6)$$

where

$$J(s_{\text{out}}, \vartheta_{\text{out}}) \equiv \left| \frac{\partial(s_{\text{in}}, \vartheta_{\text{in}})}{\partial(s_{\text{out}}, \vartheta_{\text{out}})} \right| \quad (7)$$

denotes the Jacobian of the coordinate change (5), which can be determined as follows. We introduce the coordinates $\mathbf{Q} \equiv (r, s)$, $\mathbf{P} \equiv (p_r, p_s)$ in the four dimensional phase space Γ of a single particle that are connected to the Cartesian coordinates (x, y) and the corresponding momenta (p_x, p_y) via the canonical transformation

$$x = r \cos[s/R], \quad y = r \sin[s/R], \quad p_r = m\dot{r}, \quad p_s = mr^2\dot{s}/R^2. \quad (8)$$

Next, within Γ , we define a two-dimensional surface \mathcal{S} by

$$r = \text{const} \equiv R \quad \text{and} \quad H(\mathbf{Q}, \mathbf{P}) = \text{const} \equiv E, \quad (9)$$

where $H(\mathbf{Q}, \mathbf{P})$ denotes the single particle Hamiltonian. This surface, which can be parametrized by the coordinates (s, p_s) , is pierced exactly twice by the phase space trajectory. The two intersection points $(s_{\text{in}}, p_{s_{\text{in}}})$ and $(s_{\text{out}}, p_{s_{\text{out}}})$ are connected by the one-to-one mapping

$$\mathcal{M}' : \begin{pmatrix} s_{\text{in}} \\ p_{s_{\text{in}}} \end{pmatrix} \mapsto \begin{pmatrix} s_{\text{out}}(s_{\text{in}}, p_{s_{\text{in}}}) \\ p_{s_{\text{out}}}(s_{\text{in}}, p_{s_{\text{in}}}) \end{pmatrix}. \quad (10)$$

From the Poincaré-Cartan theorem [1], it follows that the map \mathcal{M}' is volume conserving on \mathcal{S} , i.e.,

$$\left| \frac{\partial(s_{\text{in}}, p_{s_{\text{in}}})}{\partial(s_{\text{out}}, p_{s_{\text{out}}})} \right| = 1. \quad (11)$$

Rewriting (7) as

$$J(s_{\text{out}}, \vartheta_{\text{out}}) = \left| \frac{\partial(s_{\text{in}}, \vartheta_{\text{in}})}{\partial(s_{\text{in}}, p_{s_{\text{in}}})} \right| \left| \frac{\partial(s_{\text{in}}, p_{s_{\text{in}}})}{\partial(s_{\text{out}}, p_{s_{\text{out}}})} \right| \left| \frac{\partial(s_{\text{out}}, p_{s_{\text{out}}})}{\partial(s_{\text{out}}, \vartheta_{\text{out}})} \right| \quad (12)$$

leads to

$$J(s_{\text{out}}, \vartheta_{\text{out}}) = \left| \left(\frac{\partial p_{s_{\text{in}}}}{\partial \vartheta_{\text{in}}} \right)_{s_{\text{in}}} \right|^{-1} \left| \left(\frac{\partial p_{s_{\text{out}}}}{\partial \vartheta_{\text{out}}} \right)_{s_{\text{out}}} \right|. \quad (13)$$

Given the relations

$$p_{s_{\text{in}}} = \sqrt{2mE} \sin \vartheta_{\text{in}} \quad \text{and} \quad p_{s_{\text{out}}} = \sqrt{2mE} \sin \vartheta_{\text{out}}, \quad (14)$$

the partial derivatives showing up in (13) are readily calculated. Thus, we finally arrive at

$$J(s_{\text{out}}, \vartheta_{\text{out}}) = \frac{\cos \vartheta_{\text{out}}}{\cos [\vartheta_{\text{in}}(s_{\text{out}}, \vartheta_{\text{out}})]}. \quad (15)$$

Inserting this result into equation (6) gives the second sum rule (1).

We emphasize that our proof ultimately relies on the volume-preserving property of Hamiltonian dynamics and therefore applies irrespective of a potential inside the scattering region or the number of reservoirs attached to it. For simplicity, we have focused here on a circular scattering region. However, generalization to arbitrary geometries is straight forward.

Proof of Relation (18)

We will prove that the Hermitian matrix

$$\mathbb{K} \equiv \mathbb{L} + \mathbb{L}^t + i(\mathbb{L} - \mathbb{L}^t) \quad (16)$$

introduced in Eq. (17) of the main text is positive semi-definite on \mathbb{C}^2 . To this end, we need some mathematical prerequisites, which we develop first.

Definition 1. Let $\mathbb{A} \in \mathbb{R}^{n \times n}$ be positive semi-definite, then the asymmetry index of \mathbb{A} is defined as [2]

$$\mathcal{S}(\mathbb{A}) \equiv \min \{ s \in \mathbb{R} \mid \forall \mathbf{z} \in \mathbb{C}^n \quad \mathbf{z}^\dagger (s(\mathbb{A} + \mathbb{A}^t) + i(\mathbb{A} - \mathbb{A}^t)) \mathbf{z} \geq 0 \}. \quad (17)$$

Definition 2. Let $\mathbb{A} \in \mathbb{R}^{n \times n}$ be a matrix with elements $A_{ij} \equiv (\mathbb{A})_{ij} \geq 0$, then \mathbb{A} is sum-symmetric if [3]

$$\sum_i A_{ij} = \sum_i A_{ji}. \quad (18)$$

Definition 3. Let $\alpha \subseteq \{1, \dots, n\}$ be an index set and denote by $S(\alpha)$ the symmetric group on α . For any permutation $\pi \in S(\alpha)$, the matrix $\mathbb{B}(\alpha) \in \{0, 1\}^{n \times n}$ with elements

$$(\mathbb{B}(\alpha))_{ij} \equiv \begin{cases} 1 & \text{for } i, j \in \alpha \text{ and } j = \pi(i) \\ 0 & \text{else} \end{cases} \quad (19)$$

is a circuit matrix [3].

Lemma 1. For α like in Definition 3 let $\mathbb{E}(\alpha) \in \{0, 1\}^{n \times n}$ be a matrix with elements $E_{ij}(\alpha) \equiv (\mathbb{E}(\alpha))_{ij}$ such that $E_{ij} = 1$ for $i = j \in \alpha$ and $E_{ij} = 0$ otherwise. Then, for any circuit matrix $\mathbb{B}(\alpha)$, the matrix $\mathbb{E}(\alpha) - \mathbb{B}(\alpha)$ is positive semi-definite and its asymmetry index fulfills

$$\mathcal{S}(\mathbb{E}(\alpha) - \mathbb{B}(\alpha)) \leq \cot \left[\frac{\pi}{|\alpha|} \right], \quad (20)$$

where $|\alpha|$ denotes the cardinality of α .

Proof. Let $\mathbb{Q} \in \{0, 1\}^{n \times n}$ be a permutation matrix such that $\mathbb{Q}^t \mathbb{E}(\alpha) \mathbb{Q} = \mathbb{1} \oplus \mathbb{O}_{n-|\alpha|}$, where \mathbb{O}_m denotes the $m \times m$ matrix with only zero entries. Since the rows and columns of $\mathbb{B}(\alpha)$ indexed by α contain precisely one entry 1, while the remaining rows and columns contain only zero entries, we have $\mathbb{Q}^t (\mathbb{E}(\alpha) - \mathbb{B}(\alpha)) \mathbb{Q} = (\mathbb{1} - \mathbb{P}) \oplus \mathbb{O}_{n-|\alpha|}$, where $\mathbb{P} \in \{0, 1\}^{|\alpha| \times |\alpha|}$ is a permutation matrix. The matrix $\mathbb{1} - \mathbb{P}$ is positive semi-definite by virtue of Theorem 1 of Ref. [2]. Consequently, we have proven the first assertion of Lemma 1. Now, by recalling Definition 1, we find

$$\mathcal{S}(\mathbb{E}(\alpha) - \mathbb{B}(\alpha)) = \mathcal{S}(\mathbb{Q}^t (\mathbb{E}(\alpha) - \mathbb{B}(\alpha)) \mathbb{Q}) = \mathcal{S}((\mathbb{1} - \mathbb{P}) \oplus \mathbb{O}_{n-|\alpha|}) = \mathcal{S}(\mathbb{1} - \mathbb{P}) \leq \cot \left[\frac{\pi}{|\alpha|} \right], \quad (21)$$

where the last inequality again follows from Theorem 1 of Ref. [2]. \square

Corollary 1. *Let $\mathbb{A} \in \mathbb{R}^{n \times n}$ be sum-symmetric with row sums $r_i \geq 0$ and $\mathbb{D} \in \mathbb{R}^{n \times n}$ a diagonal matrix with entries $(\mathbb{D})_{ij} \equiv r_i \delta_{ij}$. Then the matrix $\mathbb{D} - \mathbb{A}$ is positive semi-definite and its asymmetry index fulfills*

$$\mathcal{S}(\mathbb{D} - \mathbb{A}) \leq \cot \left[\frac{\pi}{n} \right]. \quad (22)$$

Proof. It can be shown that for any sum-symmetric matrix \mathbb{A} there is a finite set of circuit matrices $\mathbb{B}_k(\alpha_k)$ such that

$$\mathbb{A} = \sum_k \lambda_k \mathbb{B}_k(\alpha_k), \quad (23)$$

where the λ_k are positive real numbers [3]. Accordingly, the matrix $\mathbb{D} - \mathbb{A}$ can be rewritten as

$$\mathbb{D} - \mathbb{A} = \sum_k \lambda_k (\mathbb{E}(\alpha_k) - \mathbb{B}(\alpha_k)) \quad (24)$$

with $\mathbb{E}(\alpha_k)$ like in Lemma 1. From Lemma 1, it follows that $\mathbb{D} - \mathbb{A}$ is positive semi-definite. By using the convexity of the asymmetry index, proven in Proposition 2 of Ref. [2], and again Lemma 1, we infer

$$\mathcal{S}(\mathbb{D} - \mathbb{A}) \leq \max \{ \mathcal{S}(\mathbb{E}(\alpha_k) - \mathbb{B}_k(\alpha_k)) \} \leq \max \left\{ \cot \left[\frac{\pi}{|\alpha_k|} \right] \right\} \leq \cot \left[\frac{\pi}{n} \right]. \quad (25)$$

\square

Coming back to our task of proving that the matrix (16) is positive semi-definite we consider the quadratic form

$$Q(\mathbf{z}, s) \equiv \mathbf{z}^\dagger \left(s (\mathbb{L}' + \mathbb{L}'^t) + i (\mathbb{L}' - \mathbb{L}'^t) \right) \mathbf{z} \quad (26)$$

for arbitrary $\mathbf{z} \in \mathbb{C}^8$ and

$$\mathbb{L}' \equiv \begin{pmatrix} \mathbb{L}'_{11} & \cdots & \mathbb{L}'_{14} \\ \vdots & \ddots & \vdots \\ \mathbb{L}'_{41} & \cdots & \mathbb{L}'_{44} \end{pmatrix} \equiv \int_0^\infty dE u(E) (\mathbb{D} - \mathbb{T}(E)) \otimes \begin{pmatrix} 1 & E - \mu \\ E - \mu & (E - \mu)^2 \end{pmatrix} \quad \text{with} \quad \mathbb{L}'_{ij} \equiv \begin{pmatrix} L_{ij}^{\varrho\varrho} & L_{ij}^{\varrho q} \\ L_{ij}^{q\varrho} & L_{ij}^{qq} \end{pmatrix}, \quad (27)$$

where the $L_{ij}^{\kappa\nu}$ for $\kappa, \nu = \varrho, q$ denote the primary Onsager coefficients defined in Eq. (12) of the main text. The matrix $\mathbb{T}(E) \in \mathbb{R}^{4 \times 4}$ contains the transmission coefficients $\mathcal{T}_{ij}(E)$, i.e., $(\mathbb{T}(E))_{ij} \equiv \mathcal{T}_{ij}(E)$, and $\mathbb{D} \in \mathbb{R}^{4 \times 4}$ denotes a diagonal matrix with entries $(\mathbb{D})_{ij} = 2l_i \delta_{ij}$. By putting

$$\mathbf{z} \equiv \mathbf{z}_1 \otimes \begin{pmatrix} 1 \\ 0 \end{pmatrix} + \mathbf{z}_2 \otimes \begin{pmatrix} 0 \\ 1 \end{pmatrix} \quad \text{with} \quad \mathbf{z}_1, \mathbf{z}_2 \in \mathbb{C}^4 \quad (28)$$

and inserting this decomposition as well as (27) into (26), we obtain

$$Q(\mathbf{z}, s) = \int_0^\infty dE u(E) \mathbf{y}^\dagger(E) \mathbb{K}'(s, E) \mathbf{y}(E), \quad (29)$$

where $\mathbf{y}(E) \equiv \mathbf{z}_1 + (E - \mu) \mathbf{z}_2$. The Hermitian matrix $\mathbb{K}'(s, E)$ is given by

$$\mathbb{K}'(s, E) \equiv s ((\mathbb{D} - \mathbb{T}(E)) + (\mathbb{D} - \mathbb{T}(E))^t) + i ((\mathbb{D} - \mathbb{T}(E)) - (\mathbb{D} - \mathbb{T}(E))^t) \in \mathbb{C}^4. \quad (30)$$

Comparing this expression with Definition 1 and recognizing that, thanks to the sum rules (1), Corollary 1 applies to the matrix $\mathbb{D} - \mathbb{T}(E)$ shows that $\mathbb{K}'(s, E)$ is positive semi-definite for any $s \geq \cot[\pi/4] = 1$ independent of E . Thus, since $u(E) = \sqrt{2mE} \exp[-\beta(E - \mu)]$ is non-negative for any $0 \leq E < \infty$, the quadratic form $Q(\mathbf{z}, s)$ must be positive semi-definite for $s \geq 1$ and comparing (26) with Definition 1 leads to

$$\mathcal{S}(\mathbb{L}') \leq 1. \quad (31)$$

We now construct the matrix \mathbb{L} from \mathbb{L}' in three successive steps. First, we extract the principal submatrix $\bar{\mathbb{L}}'$ by deleting the second and third row and column of \mathbb{L}' . Second, we simultaneously interchange the rows and columns of $\bar{\mathbb{L}}'$, thus transforming $\bar{\mathbb{L}}'$ to $\mathbb{P}\bar{\mathbb{L}}'\mathbb{P}^t$, where

$$\mathbb{P} \equiv \begin{pmatrix} 0 & 0 & 0 & 0 & 1 & 0 \\ 0 & 0 & 0 & 1 & 0 & 0 \\ 0 & 0 & 0 & 0 & 0 & 1 \\ 0 & 0 & 1 & 0 & 0 & 0 \\ 1 & 0 & 0 & 0 & 0 & 0 \\ 0 & 1 & 0 & 0 & 0 & 0 \end{pmatrix}. \quad (32)$$

Third, we choose the partitioning

$$\mathbb{P}\bar{\mathbb{L}}'\mathbb{P}^t \equiv \begin{pmatrix} \mathbb{M}_{11} & \mathbb{M}_{12} \\ \mathbb{M}_{21} & \mathbb{M}_{22} \end{pmatrix} \quad \text{with} \quad \mathbb{M}_{11} \equiv \begin{pmatrix} L_{44}^{ee} & L_{43}^{eq} \\ L_{34}^{qq} & L_{33}^{qq} \end{pmatrix}, \quad \mathbb{M}_{12} \equiv \begin{pmatrix} L_{44}^{eq} & L_{43}^{ee} & L_{41}^{ee} & L_{42}^{eq} \\ L_{34}^{qq} & L_{33}^{qq} & L_{31}^{qq} & L_{32}^{qq} \end{pmatrix}, \quad (33)$$

$$\mathbb{M}_{21} \equiv \begin{pmatrix} L_{44}^{qq} & L_{34}^{ee} & L_{14}^{ee} & L_{24}^{qq} \\ L_{43}^{qq} & L_{33}^{qq} & L_{13}^{qq} & L_{23}^{qq} \end{pmatrix}^t, \quad \mathbb{M}_{22} \equiv \begin{pmatrix} L_{44}^{qq} & L_{43}^{qq} & L_{41}^{qq} & L_{42}^{qq} \\ L_{34}^{qq} & L_{33}^{qq} & L_{31}^{qq} & L_{32}^{qq} \\ L_{14}^{qq} & L_{13}^{qq} & L_{11}^{qq} & L_{12}^{qq} \\ L_{24}^{qq} & L_{23}^{qq} & L_{21}^{qq} & L_{22}^{qq} \end{pmatrix} \quad (34)$$

and take the Schur complement [4] of $\mathbb{P}\bar{\mathbb{L}}'\mathbb{P}^t$ with respect to \mathbb{M}_{22} , thus ending up with

$$\mathbb{L} = \mathbb{P}\bar{\mathbb{L}}'\mathbb{P}^t / \mathbb{M}_{22} \equiv \mathbb{M}_{11} - \mathbb{M}_{12}\mathbb{M}_{22}^{-1}\mathbb{M}_{21}. \quad (35)$$

Finally, by using the Propositions 3 and 4 of Ref. [2] and the result (31), we find

$$\mathcal{S}(\mathbb{L}) = \mathcal{S}(\mathbb{P}\bar{\mathbb{L}}'\mathbb{P}^t / \mathbb{M}_{22}) \leq \mathcal{S}(\mathbb{P}\bar{\mathbb{L}}'\mathbb{P}^t) = \mathcal{S}(\bar{\mathbb{L}}') \leq \mathcal{S}(\mathbb{L}') \leq 1. \quad (36)$$

Consequently, by virtue of Definition 1, the matrix (16) must be positive semi-definite.

Calculation of the Full Transmission Coefficients (6)

In this section, we will calculate the energy dependent transmission coefficients $\mathcal{T}_{ji}(E)$, defined in Eq. (6) of the main text, for the classical Nernst engine. To this end, we consider a particle of energy E injected from the reservoir C_i with the angle ϑ at the boundary position s_{in} . After traveling through the scattering region, the particle is absorbed in the reservoir C_j at the position s_{out} . A direct geometrical analysis shows that the length $\Delta s \equiv s_{\text{out}} - s_{\text{in}}$ of the boundary segment the particle passes by is given by

$$\Delta s(\vartheta) = 2R \begin{cases} \text{arccot}[(1 + \nu \sin \vartheta)/(\nu \cos \vartheta)] + \pi & \text{for } \nu > 1, \sin \vartheta < -1/\nu \\ \text{arccot}[(1 + \nu \sin \vartheta)/(\nu \cos \vartheta)] & \text{else} \end{cases}, \quad (37)$$

where

$$\nu \equiv R_c/R = \sqrt{E/\varepsilon} \quad \text{with} \quad \varepsilon \equiv q^2 B^2 R^2 / (2mc^2). \quad (38)$$

For $\nu \leq 1$, $\Delta s(\vartheta)$ has a global maximum

$$\Delta s^* \equiv 2R \text{arccot} \left[\sqrt{1 - \nu^2} / \nu \right] = 2R \arcsin \nu \leq \pi R, \quad (39)$$

with respect to ϑ , which it assumes for $\sin \vartheta = -\nu$. For $\nu > 1$, $\Delta s(\vartheta)$ captures the whole interval $[0, 2\pi R)$ as ϑ runs from $-\pi/2$ to $\pi/2$. In both bases, we can solve (37) for $\sin \vartheta$, thus obtaining

$$\sin[\vartheta_{\pm}(\Delta s)] = h_{\pm}(\Delta s) \quad \text{for } \nu \leq 1 \quad \text{and} \quad \sin[\vartheta_{+}(\Delta s)] = h_{+}(\Delta s) \quad \text{for } \nu > 1 \quad (40)$$

with

$$h_{\pm}(x) \equiv (1/\nu) \left(-\sin^2 [x/(2R)] \pm \cos [x/(2R)] \sqrt{\nu^2 - \sin^2 [x/(2R)]} \right). \quad (41)$$

Using this result, a reflection coefficient with rescaled argument defined as $\bar{\mathcal{T}}_{ii}(\nu) \equiv \mathcal{T}_{ii}(E(\nu)) = \mathcal{T}_{ii}(\varepsilon\nu^2)$ can be written as

$$\bar{\mathcal{T}}_{ii}(\nu) = \begin{cases} \int_0^{l_i} d\sigma_i \int_{-\pi/2}^{\pi/2} d\vartheta \cos \vartheta - \int_0^{\Delta s^*} d\sigma_i \int_{\vartheta_-(\sigma_i)}^{\vartheta_+(\sigma_i)} d\vartheta \cos \vartheta & \text{for } \nu \leq \alpha_i \\ \int_0^{l_i} d\sigma_i \int_{-\pi/2}^{\pi/2} d\vartheta \cos \vartheta - \int_0^{l_i} d\sigma_i \int_{\vartheta_-(\sigma_i)}^{\vartheta_+(\sigma_i)} d\vartheta \cos \vartheta & \text{for } \alpha_i < \nu \leq 1 \\ \int_0^{l_i} d\sigma_i \int_{\vartheta_+(2\pi R)}^{\vartheta_+(\sigma_i+2\pi R-l_i)} d\vartheta \cos \vartheta + \int_0^{l_i} d\sigma_i \int_{\vartheta_+(\sigma_i)}^{\vartheta_+(0)} d\vartheta \cos \vartheta & \text{for } 1 < \nu. \end{cases} \quad (42)$$

with $\alpha_i \equiv \sin[l_i/(2R)]$ and $\sigma_i \equiv s_i - s_{\text{in}}$ (see Fig. 1 of the main text for the definition of s_i). The integrals showing up in (42) can be solved by standard techniques giving

$$\bar{\mathcal{T}}_{ii}(\nu) = \begin{cases} 2l_i - \pi R\nu & \text{for } \nu \leq \alpha_i \\ 2l_i - 2H(\alpha_i, \nu) & \text{for } \alpha_i < \nu \end{cases} \quad (43)$$

with

$$H(\alpha, \nu) \equiv R \left((\alpha/\nu) \sqrt{\nu^2 - \alpha^2} + \nu \arcsin[\alpha/\nu] \right). \quad (44)$$

Analogously, we can express the $\bar{\mathcal{T}}_{i+1i}(\nu)$. Using $l_i + l_{i+1} = \pi R$, we obtain

$$\bar{\mathcal{T}}_{i+1i}(\nu) \equiv \mathcal{T}_{i+1i}(\varepsilon\nu^2) = \begin{cases} \int_0^{\Delta s^*} d\sigma_i \int_{\vartheta_-(\sigma_i)}^{\vartheta_+(\sigma_i)} d\vartheta \cos \vartheta & \text{for } \nu \leq \alpha_i \\ \int_0^{l_i} d\sigma_i \int_{\vartheta_-(\sigma_i)}^{\vartheta_+(\sigma_i)} d\vartheta \cos \vartheta & \text{for } \alpha_i < \nu \leq \alpha_{i+1} \\ \int_0^{l_i} d\sigma_i \int_{\vartheta_-(\sigma_i)}^{\vartheta_+(\sigma_i)} d\vartheta \cos \vartheta - \int_0^{\Delta s^* - l_{i+1}} d\sigma_i \int_{\vartheta_-(\sigma_i+l_{i+1})}^{\vartheta_+(\sigma_i+l_{i+1})} d\vartheta \cos \vartheta & \text{for } \alpha_{i+1} < \nu \leq 1 \\ \int_0^{l_i} d\sigma_i \int_{\vartheta_+(\sigma_i+l_{i+1})}^{\vartheta_+(\sigma_i)} d\vartheta \cos \vartheta & \text{for } 1 < \nu \end{cases} \quad (45)$$

for $l_i \leq l_{i+1}$ and

$$\bar{\mathcal{T}}_{i+1i}(\nu) = \begin{cases} \int_0^{\Delta s^*} d\sigma_i \int_{\vartheta_-(\sigma_i)}^{\vartheta_+(\sigma_i)} d\vartheta \cos \vartheta & \text{for } \nu \leq \alpha_{i+1} \\ \int_0^{\Delta s^*} d\sigma_i \int_{\vartheta_-(\sigma_i)}^{\vartheta_+(\sigma_i)} d\vartheta \cos \vartheta - \int_0^{\Delta s^* - l_{i+1}} d\sigma_i \int_{\vartheta_-(\sigma_i+l_{i+1})}^{\vartheta_+(\sigma_i+l_{i+1})} d\vartheta \cos \vartheta & \text{for } \alpha_{i+1} < \nu \leq \alpha_i \\ \int_0^{l_i} d\sigma_i \int_{\vartheta_-(\sigma_i)}^{\vartheta_+(\sigma_i)} d\vartheta \cos \vartheta - \int_0^{\Delta s^* - l_{i+1}} d\sigma_i \int_{\vartheta_-(\sigma_i+l_{i+1})}^{\vartheta_+(\sigma_i+l_{i+1})} d\vartheta \cos \vartheta & \text{for } \alpha_i < \nu \leq 1 \\ \int_0^{l_i} d\sigma_i \int_{\vartheta_+(\sigma_i+l_{i+1})}^{\vartheta_+(\sigma_i)} d\vartheta \cos \vartheta & \text{for } 1 < \nu \end{cases} \quad (46)$$

for $l_i > l_{i+1}$. Evaluating the integrals yields

$$\bar{\mathcal{T}}_{i+1i}(\nu) = \begin{cases} \pi R\nu & \text{for } \nu \leq \alpha_i^{\min} \\ 2H(\alpha_i^{\min}, \nu) & \text{for } \alpha_i^{\min} < \nu \leq \alpha_i^{\max} \\ 2H(\alpha_i^{\min}, \nu) + 2H(\alpha_i^{\max}, \nu) - \pi R\nu & \text{for } \alpha_i^{\max} < \nu \leq 1 \\ H(\alpha_i^{\min}, \nu) + H(\alpha_i^{\max}, \nu) - H(1, \nu) + (R/\nu) \sin[l_i/R] & \text{for } 1 < \nu \end{cases}, \quad (47)$$

where $\alpha_i^{\min} \equiv \min\{\alpha_i, \alpha_{i+1}\}$ and $\alpha_i^{\max} \equiv \max\{\alpha_i, \alpha_{i+1}\}$. Finally, we calculate

$$\bar{\mathcal{T}}_{i+2i}(\nu) \equiv \mathcal{T}_{i+2i}(\varepsilon\nu^2) = \begin{cases} 0 & \text{for } \nu \leq \alpha_{i+1} \\ \int_0^{\Delta s^* - l_{i+1}} d\sigma_i \int_{\vartheta_-(\sigma_i+l_{i+1})}^{\vartheta_+(\sigma_i+l_{i+1})} d\vartheta \cos \vartheta & \text{for } \alpha_{i+1} < \nu \leq 1 \\ \int_0^{l_i} d\sigma_i \int_{\vartheta_+(\sigma_i+\pi R)}^{\vartheta_+(\sigma_i+l_{i+1})} d\vartheta \cos \vartheta & \text{for } 1 < \nu \end{cases} \quad (48)$$

$$= \begin{cases} 0 & \text{for } \nu \leq \alpha_{i+1} \\ \pi R\nu - 2H(\alpha_{i+1}, \nu) & \text{for } \alpha_{i+1} < \nu \leq 1 \\ 2H(1, \nu) - 2H(\alpha_{i+1}, \nu) & \text{for } 1 < \nu \end{cases} \quad (49)$$

and

$$\bar{\mathcal{T}}_{i+3i}(\nu) \equiv \mathcal{T}_{i+3i}(\varepsilon\nu^2) = \begin{cases} 0 & \text{for } \nu \leq 1 \\ \int_0^{l_i} d\sigma_i \int_{\vartheta_+(\sigma_i+2\pi R-l_i)}^{\vartheta_+(\sigma_i+\pi R)} d\vartheta \cos \vartheta & \text{for } 1 < \nu \end{cases} \quad (50)$$

$$= \begin{cases} 0 & \text{for } \nu \leq 1 \\ H(\alpha_{i+1}, \nu) + H(\alpha_i, \nu) - H(1, \nu) - (R/\nu) \sin[l_i/R] & \text{for } 1 < \nu \end{cases}. \quad (51)$$

We note that the sum rules

$$\sum_i \bar{\mathcal{T}}_{ji} = \sum_i \mathcal{T}_{ji} = 2l_j \quad \text{and} \quad \sum_j \bar{\mathcal{T}}_{ji} = \sum_j \mathcal{T}_{ji} = 2l_i \quad (52)$$

are easily verified for the coefficients (43), (47), (49) and (51).

-
- [1] E. Ott, *Chaos in Dynamical Systems*, 2nd ed. (Cambridge University Press, 2002).
 - [2] K. Brandner and U. Seifert, arXiv:1308.2179v1, *New J. Phys.*, in press (2013).
 - [3] R. B. Bapat and T. E. S. Raghavan, *Nonnegative Matrices and Applications*, 1st ed. (Cambridge University Press, 2009).
 - [4] F. Zhang, *The Schur Complement and its Applications*, 1st ed. (Springer, 2005).